

## Polarization effects in Compton scattering

This article has been downloaded from IOPscience. Please scroll down to see the full text article.

1968 J. Phys. A: Gen. Phys. 1 251

(<http://iopscience.iop.org/0022-3689/1/2/309>)

View [the table of contents for this issue](#), or go to the [journal homepage](#) for more

Download details:

IP Address: 129.252.86.83

The article was downloaded on 30/05/2010 at 13:37

Please note that [terms and conditions apply](#).

## Polarization effects in Compton scattering

A. S. RAJU, J. RAMA RAO and V. LAKSHMINARAYANA

Laboratories for Nuclear Research, Andhra University, Waltair, India

*MS. received 21st June 1966, in revised form 29th November 1967*

**Abstract.** An experimental investigation has been made of the polarization effects in the inelastic scattering of 662 keV photons from a 10 Ci  $^{137}\text{Cs}$  source, using a polarization analyser equipped with sum-coincidence arrangement. The experiments were conducted at four scattering angles ( $45^\circ$ ,  $60^\circ$ ,  $75^\circ$  and  $90^\circ$ ) and three azimuthal angles ( $30^\circ$ ,  $60^\circ$  and  $90^\circ$ ). The coincidence rates in two different planes were collected simultaneously. The results are in satisfactory agreement with the predictions of the Klein-Nishina theory.

### 1. Introduction

The inelastic scattering of photons by free electrons is described by the Klein-Nishina theory, which predicts a partial polarization of the scattered beam. Although numerous investigations (Evans 1958) have been made on the differential as well as integral cross sections confirming the theory, relatively few investigations have been carried out on the polarization effects, which provide a more sensitive test of the theory. The polarization effects in inelastic scattering were studied experimentally by two groups of investigators, Hoover *et al.* (1952) and Singh *et al.* (1965). Hoover and collaborators employed a  $^{60}\text{Co}$  source to provide primary gamma rays of mean energy 1250 keV, and measured the azimuthal variations of the secondary scattered gamma rays at  $90^\circ$  for primary scattering angles of  $83^\circ$  and  $50^\circ$ . Although the results indicated a general agreement with theory, there were appreciable deviations at certain azimuthal angles. Singh and collaborators conducted similar experiments for primary scattering angles of  $64^\circ$ ,  $90^\circ$  and  $120^\circ$  using primary photons of energies 280, 662 and 1250 keV. They reported better agreement of their results with theory than those of Hoover *et al.* Both these investigations employed a similar experimental arrangement with two scintillation detectors in coincidence. The scattering events in an azimuthal plane were selected by a coincidence method, and the asymmetry ratio  $N_0/N_\phi$  was determined by observing the coincidence count rates  $N_0$  and  $N_\phi$  successively. The source intensities employed by them were small, resulting in poor counting statistics. It was therefore felt desirable to collect some more information in this direction under improved experimental conditions. In the present investigation a 10 Ci source of  $^{137}\text{Cs}$  was used to improve the counting statistics. Statistical superiority was achieved by observing the count rates  $N_0$  and  $N_\phi$  in the two azimuthal planes simultaneously, which also helped to minimize the effects due to electronic drifts to a great extent. In the place of a simple coincidence arrangement used by them, a sum coincidence arrangement was used to determine the asymmetry ratios  $R (= N_0/N_\phi)$  at azimuthal angles  $\phi = 30^\circ$ ,  $60^\circ$  and  $90^\circ$ , for the primary scattering angles of  $45^\circ$ ,  $60^\circ$ ,  $75^\circ$  and  $90^\circ$ .

### 2. Experimental details

The source (10 Ci  $^{137}\text{Cs}$ ) was contained in the axial hole, diameter 1 in., of a mild-steel cylinder, 2 ft diam.  $\times$  2 ft high, filled with lead. It was held by a phosphor-bronze clip at the end of a lead-filled brass tube of external diameter 1 in., moving smoothly in the axial hole of the source holder, and its position could be easily adjusted. Between the source and the end of the source holder towards the target side provision was made to collimate the gamma rays. The collimation consisted of a lead-filled brass tube 6 in. in length with a tapered hole in it, the interior and exterior opening diameters being  $\frac{1}{4}$  in. and  $\frac{3}{4}$  in. respectively. The collimated beam of gamma rays was scattered by an aluminium target placed at a distance of 13 in. from the source. The target was in the form of a right circular cylinder,  $\frac{1}{2}$  in. diam.  $\times$   $\frac{1}{2}$  in. high, and was supported on a Perspex target holder, with its circular cross section resting on the target holder. The scattered beam from

the target was further collimated by the axial hole of diameter 1 in. in a lead-filled mild-steel cylinder of similar structure to that of the source holder and of dimensions 1 ft diam.  $\times$  1 ft high, the distance of its front face being 3 in. from the target. The collimated scattered beam of gamma rays was incident on the central NaI(Tl) crystal of dimensions 1 in. diam.  $\times$  1 in. high, placed at 3 in. from the far end of the collimator. Thus the distance of the front face of the central NaI(Tl) crystal from the target was 18 in. However, for angles of primary scattering of  $60^\circ$  and  $45^\circ$  this distance was increased to 22 in. in order to prevent any part of the collimator intercepting the primary beam. The secondary scattered gamma rays from the central NaI(Tl) crystal were received by two other NaI(Tl) crystals of dimensions  $1\frac{1}{2}$  in. diam.  $\times$  1 in. high, placed at different azimuthal angles—one placed at a fixed azimuthal angle  $\phi = 0$  and the other at an angle  $\phi$  which could be varied. Each of these crystals was coupled to a DuMont 6292 photomultiplier and the three detectors were connected in two sum-coincidence arrangements, as shown in figure 1.

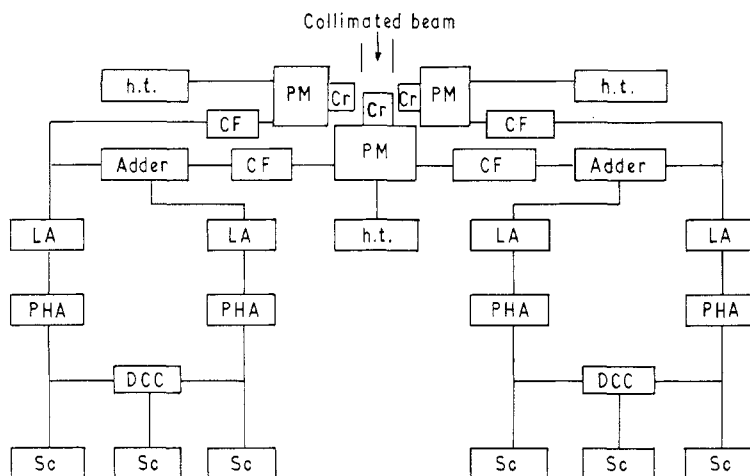


Figure 1. Block diagram of the electronic assembly: PM, photomultiplier; Cr, NaI (Tl) crystal; h.t., high tension; CF, cathode follower; LA, linear amplifier; PHA, pulse-height analyser; DCC, double-coincidence circuit; Sc, scaler.

Under these conditions the added spectrum in each spectrometer showed a prominent peak at the sum energy, which enabled an accurate setting of the gate. The sum-coincidence spectrum showed a prominent peak only at the scattered photon energy of interest. Typical spectra are shown in figures 2 and 3. To determine the asymmetry ratio  $R$ , channels of suitable width were symmetrically fixed about the peaks of the sum-coincidence spectra in each spectrometer and the coincidence rates  $N_0$  and  $N_\phi$  were obtained simultaneously.

Auxiliary experiments were conducted to study the diffuse background and, at all angles investigated, suitable additional shielding material (lead) was employed to bring down the level of diffuse background to about the same level. Auxiliary experiments were conducted to choose the optimum size of the scatterer (aluminium) to yield as large an intensity as possible without giving rise to excessive multiple scattering. The size of the scatterer thus selected was of dimensions  $\frac{1}{2}$  in. diam.  $\times$   $\frac{1}{2}$  in. high. Intrinsic asymmetry in the experimental set-up and the collimator scattering effects were also investigated. The intrinsic asymmetry was studied by replacing the central crystal by a source of  $^{114m}\text{In}$  and found to be small. To correct for the residual intrinsic asymmetry, the asymmetry ratio in each case was determined by interchanging the scintillation counters in the azimuthal and horizontal planes. The corresponding asymmetry ratios  $R'$  and  $R''$  were employed to obtain the correct asymmetry ratio as  $R = (R'R'')^{1/2}$ . To investigate the collimator scattering effects, a source of unpolarized photons was used to determine the

asymmetry ratio. For this purpose, the source radiation was blocked and a source of  $^{203}\text{Hg}$  was placed in the target position. (The energy of photons from  $^{203}\text{Hg}$ , 279 keV, corresponds to the primary scattered photon energy at  $90^\circ$ .) The asymmetry ratio, determined several times, did not differ appreciably from unity, indicating the collimator

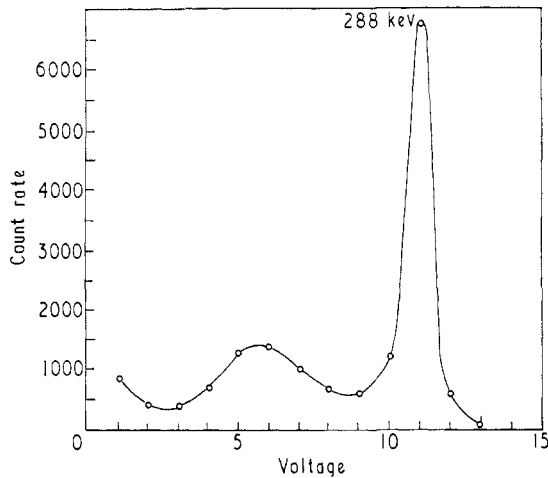


Figure 2. Added spectrum at a primary scattering angle of  $90^\circ$ .

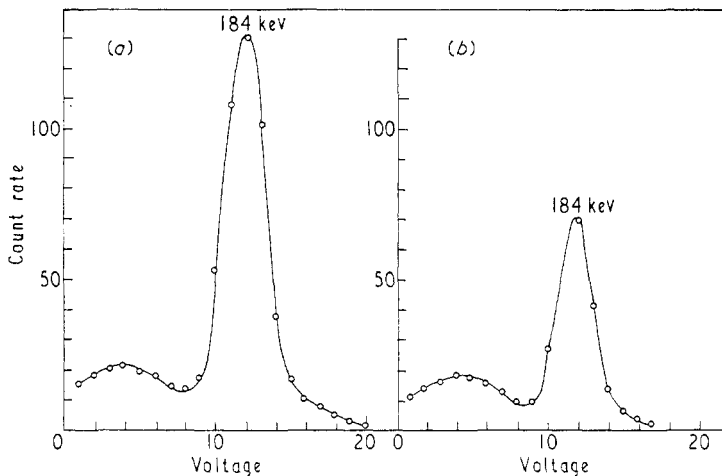


Figure 3. Sum-coincidence spectra at a primary scattering angle of  $90^\circ$ : (a) counter at  $\phi = 0^\circ$ ; (b) counter at  $\phi = 90^\circ$ .

scattering effects to be negligible. The effect of collimator scattering for the primary source holder influenced the present experimental studies in a secondary manner. The opening of the collimator of the source holder was such as to produce a beam of cross section in the target position larger than the target dimensions, so that the ratio of the number of unscattered to scattered photons in the collimator traversing the target was high. The effect was therefore disregarded.

In the present study narrow gates about the peaks in the spectra were set, and an intense source of primary photons (10 Ci  $^{137}\text{Cs}$ ) was employed. This resulted in a better true-to-chance ratio compared with the two earlier investigations. A total of 2000 coincidence counts were collected in each experimental run, and the experimental times were much shorter compared with those of the earlier investigators, so that systematic errors

due to electronic drifts were quite small. From the total coincidence rate, the chance and false coincidence rates were subtracted. The chance coincidences were due to the finite resolving time of the coincidence arrangement and were estimated from the known resolving time ( $2\tau = 3 \mu\text{s}$  in the present case) and singles counts. They were about 4% of the gross coincidence counts. The false coincidences resulted from the background effects and contributions by the target mount. They were determined by conducting 'blank experiments' with no target on the target holder for a time equal to the experimental time with the target. They were found to be of the order of 6% of the gross coincidence counts. As such, it can be said that a signal-to-noise ratio of 9 was achieved in the present work. Taking into account the relative statistical errors and their combined effect in the final asymmetry ratio, we found that the overall error in the experimental determination did not exceed 5%.

### 3. Theoretical calculations

In the notation adopted earlier (Singh *et al.* 1965) the asymmetry ratio  $R$  at an azimuthal angle  $\phi$  (defined as  $N_0/N_\phi$ , where  $N_0$  and  $N_\phi$  are the count rates at azimuthal angles  $0^\circ$  and  $\phi^\circ$  respectively) is computed using the formulae

$$R = \frac{N_0}{N_\phi} = \frac{1 + PR_1}{PR_2 + R_3} \quad (1)$$

$$P = \frac{\int_{\Delta\theta_1} \int_{\Delta\phi_1} d\sigma_1(\theta_1, \phi_1)_{\phi_1 = 0^\circ}}{\int_{\Delta\theta_1} \int_{\Delta\phi_1} d\sigma_1(\theta_1, \phi_1)_{\phi_1 = 90^\circ}} \quad (2)$$

$$R_1 = \frac{\int_{\Delta\theta_2} \int_{\Delta\phi_2} d\sigma_2(\theta_2, \phi_2)_{\phi_2 = 0^\circ}}{\int_{\Delta\theta_2} \int_{\Delta\phi_2} d\sigma_2(\theta_2, \phi_2)_{\phi_2 = 90^\circ}} \quad (3)$$

$$R_2 = \frac{\int_{\Delta\theta_2} \int_{\Delta\phi_2} d\sigma_2(\theta_2, \phi_2)_{\phi_2 = \phi}}{\int_{\Delta\theta_2} \int_{\Delta\phi_2} d\sigma_2(\theta_2, \phi_2)_{\phi_2 = 90^\circ}} \quad (4)$$

$$R_3 = \frac{\int_{\Delta\theta_2} \int_{\Delta\phi_2} d\sigma_2(\theta_2, \phi_2)_{\phi_2 = 90^\circ - \phi}}{\int_{\Delta\theta_2} \int_{\Delta\phi_2} d\sigma_2(\theta_2, \phi_2)_{\phi_2 = 90^\circ}} \quad (5)$$

In the above equations  $d\sigma_1$  and  $d\sigma_2$  are the differential Klein-Nishina cross sections for the primary and secondary scattering respectively and  $\Delta\theta_1$ ,  $\Delta\phi_1$  and  $\Delta\theta_2$ ,  $\Delta\phi_2$  are the angular ranges involved in the geometry. For the primary scattering the angular ranges  $\Delta\theta_1$  and  $\Delta\phi_1$  vary between  $4^\circ$  and  $6^\circ$  for the various scattering angles. For the secondary scattering, however,  $\Delta\theta_2$  and  $\Delta\phi_2$  are approximately constant at all primary angles of scattering. The theoretical values of the asymmetry ratios were obtained by numerical integration of equations (2) to (5) over  $\Delta\theta$  and analytical integration over  $\Delta\phi$ . These estimates were also made by numerical integration over both  $\Delta\theta$  and  $\Delta\phi$ . The values obtained in a number of trials revealed that an error of the order of 5% might be involved.

**Table 1. Theoretical and experimental asymmetry ratios**

$\theta_1$ (deg)	$R = N_0/N_{30}$	$R = N_0/N_{60}$	$R = N_0/N_{90}$
45 Exp.	$0.99 \pm 0.05$	$1.19 \pm 0.06$	$1.32 \pm 0.07$
Theor.	$1.10 \pm 0.05$	$1.32 \pm 0.07$	$1.46 \pm 0.07$
60 Exp.	$1.03 \pm 0.05$	$1.43 \pm 0.07$	$1.76 \pm 0.09$
Theor.	$1.14 \pm 0.06$	$1.57 \pm 0.08$	$1.96 \pm 0.10$
75 Exp.	$1.05 \pm 0.05$	$1.61 \pm 0.08$	$2.22 \pm 0.11$
Theor.	$1.17 \pm 0.06$	$1.79 \pm 0.09$	$2.44 \pm 0.12$
90 Exp.	$1.05 \pm 0.05$	$1.49 \pm 0.08$	$1.91 \pm 0.10$
Theor.	$1.15 \pm 0.06$	$1.64 \pm 0.08$	$2.09 \pm 0.10$

#### 4. Results and discussion

The experimental and theoretical values of the asymmetry ratios for the three azimuthal angles at each of the primary scattering angles are given in table 1. It can be seen from the values given in table 1 that the mean theoretical and experimental values differ by about 10% at all azimuthal angles and primary scattering angles. Since the experimental and theoretical errors are each of the order of 5%, the agreement appears to be satisfactory. However, the theoretical values have to be corrected for two effects—relative weightings for detection at different angles involved in the numerical integrations, and the deviation of the effective solid angle from the one determined by geometry. Auxiliary experiments were conducted to determine the relative photopeak efficiencies for the two side channels, using a method described by Frankel (1951) in the energy and angular ranges involved in the present experiment. These relative photopeak efficiencies were employed in the numerical integrations to obtain the theoretical values. The weighted theoretical values were found to be larger than the unweighted ones. But, taken together with the enhanced errors, no substantial deviation in the values was noticed. The effect of a possible deviation of the effective solid angle from the geometric one was also investigated for assumed differences up to 5°. These deviations were observed to produce a change in theoretical values by about 1%. It is therefore concluded that the Klein–Nishina theory predicts the polarization effects in Compton scattering accurately at least in first order.

#### References

- EVANS, R. D., 1958, *Encyclopaedia of Physics*, **34**, 218–97, Ed. S. Flügge (Berlin: Springer-Verlag).  
FRANKEL, S., 1951, *Phys. Rev.*, **83**, 673.  
HOOVER, J. I., FAUST, W. R., and DOHNE, C. F., 1952, *Phys. Rev.*, **85**, 58–9.  
SINGH, M., ANAND, S., and SOOD, B. S., 1965, *Nucl. Phys.*, **62**, 267–72.